Water Research 147 (2018) 321–330

Contents lists available at ScienceDirect

Water Research

journal homepage: www.elsevier.com/locate/watres

Highly effective oxidation of roxarsone by ferrate and simultaneous arsenic removal with *in situ* formed ferric nanoparticles

Tao Yang [a], Yulei Liu [b], Lu Wang [a, *], Jin Jiang [a], Zhuangsong Huang [a], Su-Yan Pang [c], Haijun Cheng [a], Dawen Gao [a], Jun Ma [a, **]

[a] State Key Laboratory of Urban Water Resource and Environment, School of Municipal and Environmental Engineering, Harbin Institute of Technology, Harbin, 150090, China
[b] Technology R & D Center for Environmental Engineering, Dongguan University of Technology, Dongguan, 523808, China
[c] School of Municipal and Environmental Engineering, Jilin Jianzhu University, Changchun, 130118, China

ARTICLE INFO

Article history:
Received 24 May 2018
Received in revised form
8 September 2018
Accepted 4 October 2018
Available online 7 October 2018

Keywords:
Roxarsone
Ferrate
Arsenic(III)
Arsenic(V)
Ferric nanoparticles

ABSTRACT

Roxarsone (ROX) is used in breeding industry to prevent infection by parasites, stimulate livestock growth and improve pigmentation of livestock meat. After being released into environment, ROX could be bio-degraded with the formation of carcinogenic inorganic arsenic (As) species. Here, ferrate oxidation of ROX was reported, in which we studied total-As removal, determined reaction kinetics, identified oxidation products, and proposed a reaction mechanism. It was found that the apparent second-order rate constant (k_{app}) of ferrate with ROX was 305 $M^{-1}s^{-1}$ at pH 7.0, 25 °C, and over 95% of total As was removed within 10 min when ferrate/ROX molar ratio was 20:1. Species-specific rate constants analysis showed that $HFeO_4^-$ was the dominant species reacting with ROX. Ferrate initially attacked As—C bond of ROX and resulted in the formation of arsenate and 2-nitrohydroquinone. The arsenate was simultaneously removed by ferric nanoparticles formed in the reduction of ferrate, while 2-nitrohydroquinone was further oxidized into nitro-1,4-benzoquinone. These results suggest that ferrate treatment can be an effective method for the control of ROX in water treatment.

1. Introduction

Due to increasing demand for meat, breeding industry has become one of the fastest growing agricultural sectors in the past decades. (Thornton, 2010). In order to increase production's efficiency and improve product quality, veterinary drugs and feed additives are extensively utilized (Sarmah et al., 2006). Roxarsone (ROX, 3-nitro-4-hydroxybenzene arsonic acid) is used to prevent infection by parasites, stimulate livestock growth and improve pigmentation of livestock meat (Chapman and Johnson, 2002). ROX is poorly metabolized by livestock, and large amount of consumed ROX is excreted in original form through animal feces (Liu et al., 2015; Stolz et al., 2007). Although ROX is not highly toxic to humans, it could be transformed via biotic and abiotic pathways in the environment (Han et al., 2017) and release carcinogenic inorganic arsenic (As) species (Hu et al., 2017). Studies estimated that every year thousands of tons of ROX are consumed worldwide (Guo et al., 2013). Extensive use, wide distribution and potential toxicity have rendered ROX a severe threat to the ecosystem and human health.

Different treatment methods such as physical adsorption (Chen and Huang, 2012; Joshi et al., 2017b; Li et al., 2016; Tian et al., 2017), advanced oxidation (Hu et al., 2015; Ji et al., 2016), and photodegradation (Adak et al., 2015; Bednar et al., 2003; Xie et al., 2016) have been investigated for the removal of ROX in aqueous solution. Adsorbents such as Fe_3O_4@RGO nanocomposite (Tian et al., 2017), Fe—Mn binary oxides (Joshi et al., 2017b), and iron and aluminum oxides (Chen and Huang, 2012) have shown great results for ROX removal. However, organoarsenic compounds are difficult to be removed through adsorption process as compared with inorganic arsenic, and the time to achieve desired adsorption equilibrium is normally more than 5 h. Considering that ROX mainly existing at ppb to ppm level in environmental samples (Garbarino et al., 2003), long adsorption time would lead to the application of large amount of adsorbent and prolonging hydraulic retention time. ROX can be oxidized by heat activated persulfate, and the ROX removal

* Corresponding author.
** Corresponding author.
E-mail addresses: wanglu9195@163.com (L. Wang), majun@hit.edu.cn (J. Ma).

https://doi.org/10.1016/j.watres.2018.10.012
0043-1354/

efficiency increased from 11% to 98% as the temperature increased from 40 to 70 °C in the reaction time of 8 h (Ji et al., 2016). Hu et al. reported that Fenton enhanced plasma system could oxidize ROX (Hu et al., 2015), yet the reaction is highly pH-dependent and has to be proceeded under acidic conditions. The released arsenic species could be immobilized by ferric oxyhydroxides at pH 4.0–6.0 as the initial concentration of Fe(II) ranged from 500 to 1000 μM.

Ferrate [Fe(VI)] is an environmental friendly oxidant (Lee et al., 2005; Ma and Liu, 2002; Sharma, 2002) and is investigated for the treatment of emerging pollutants (Feng et al., 2016; Yang and Ying, 2013), odor compounds (He et al., 2009; Liu et al., 2018a), heavy metals (Jiang, 2007; Lee et al., 2003a), and aquatic microbes (Fan et al., 2018). As a strong oxidant, ferrate tends to attack electron-rich organic moieties such as phenols, organosulfur compounds, nitrogen-containing compounds, and pharmaceuticals (Graham et al., 2004; Sharma et al., 2001; Yang et al., 2012). Meanwhile, *in-situ* formed ferric nanoparticles generated in the ferrate reduction process have a great potential to remove hazardous ions such as As(III) (Lee et al., 2003a; Prucek et al., 2013) from water. Since ROX contains electron-rich moieties and the released As species may be simultaneously removed by the ferrate resultant ferric nanoparticles, the effectiveness of ferrate treatment on ROX removal and total-As control aroused our interest.

Herein, the oxidation kinetics and reaction mechanism of ROX with ferrate was investigated. Reaction kinetics were examined in buffered waters at pH 6.5 to pH 10, and species-specific reactions between ferrate species and ROX species were analyzed. Transformation of As species during the oxidation process was examined, and removal of total-As was determined. To fully understand reaction mechanism, liquid chromatography-mass spectrometric analysis was employed to study transformation products, and ROX transformation pathway was proposed. Aggregation behavior of ferrate resultant particles, desorption of As from settled floc, and effects of ferrate treatment on ROX oxidation and total-As removal in authentic waters were investigated as well.

2. Materials and methods

2.1. Chemicals and reagents

ROX (98% purity) was purchased from Tokyo Chemical Industry (Japan) and dissolved in pure water as stock solution (1 mM). Other chemicals are of analytical grade and directly used as received. Potassium ferrate (K_2FeO_4) was prepared according to previously described method (Liu et al., 2016). Briefly, KOH reacted with chlorine gas to form KClO solution. Subsequently, pulverized $Fe(NO_3)_3\,9H_2O$ was added into the solution and reacted at 30 °C for over 90 min. KOH (20 g) was then added under cooling condition (<5 °C), and stirred for 30 min. The newly formed slurry was filtered through a glass filter, and the precipitate was rinsed with 30 mL of 1 M aqueous KOH solution under cooling condition (<2 °C). The filtrate was collected and added to a beaker containing 300 mL cooled saturated KOH solution. The mixture was stand for 10 min and then filtered with a glass filter (P-3), followed by double filtering with GF/A filter papers (Whatman ∅ 47 mm). The precipitate was rinsed with n-hexane (4 times × 20 mL), n-pentane (4 times × 20 mL), methanol (4 times × 20 mL), and diethyl ether (4 times × 20 mL). Prior to use, the K_2FeO_4 powder (purity: > 85%) was dissolved in 1 mM Na_2CO_3 solution (pH = 9.2), and swiftly filtered through a hydrophilic acetate fiber membrane of 0.22 μm pore size (Shanghai ANPEL, China). The concentration of K_2FeO_4 was determined with a UV–Visible spectrophotometry at 510 nm with $\varepsilon_{510nm} = 1150\ cm^{-1}M^{-1}$ (Rush and Bielski, 1986). After calculation, defined amount of K_2FeO_4 stock solution was swiftly added into the reactors.

2.2. Water samples

Three water samples were used in the study. River water was collected from Songhua River of Harbin, China. Ground water was collected from a well in Harbin Institute of Technology, Heilongjiang province, China. Waste water treatment plant (WWTP) effluent water was collected from the secondary settling tank of Harbin WenChang municipal WWTP. Water samples were filtered through a glass-fiber membrane of 0.75 μm pore size and stored at 4 °C prior to use. The properties of water samples are listed in Table 1.

2.3. Experimental procedures

ROX concentration was determined with high-performance liquid chromatography (HPLC, Waters 2695) with a symmetry C18 column (4.6 × 150 mm, 5 μm particle size, Waters) and a photodiode array detector (PDA, Waters 2998) at wavelength of 264 nm. The mobile phase consisted of methanol and water (1‰ (v/v) acetic acid) at a ratio of 20:80 (v/v), and a flow rate of 1.0 mL min^{-1} was used. Concentration of inorganic As species was determined on an inductively coupled plasma mass spectrometer (ICP-MS, NexION 300Q, Perkin-Elmer) with a HPLC. Separation of arsenite and arsenate was achieved on a Hamilton PRP-X100 anion exchange chromatographic column (5 μm, 4.6 × 250 mm). The mobile phase consisted of 50 mM $(NH_4)_2HPO_4$ solution (pH adjusted to 5.4 with HNO_3) and water at a ratio of 80:20 (v/v), and a flow rate of 1.5 mL min^{-1} was applied. In the experiment, definite amount of ROX stock solution was added into glass beakers containing 500 mL of 10 mM $NaHCO_3$ solution, and the pH value was adjusted to 7.0 by adding 0.1 M HCl or NaOH. Then K_2FeO_4 solution was added into the beakers to start reaction. Water samples were taken at different time intervals and filtered through hydrophilic acetate fiber membrane of 0.22 μm pore size (Shanghai ANPEL, China).

2.4. Reaction kinetics study

Oxidation experiment was carried in 200 mL beaker equipped with a magnetic stirrer (500 r/min) at 25.0 ± 0.2 °C. Solution pH was buffered with 20 mM borate buffer (adjusted by 1 M HCl or 1 M NaOH from pH 6.5 to 10.0). Reactions were started by adding an aliquot of ferrate stock solution (filtered and standardized) to the ROX solution under rapid mixing condition. At different time intervals, 1.0 mL of the solution was sampled and swiftly added into a 2.0 mL vial containing 10 μL of 700 mM hydroxylamine hydrochloride to quench the reaction. Oxidation kinetics of ROX with ferrate were fitted with second-order reaction rate law [Eq (1)].

Table 1
The characteristics of authentic water samples.

	River water	Ground water	WWTP effluent
TOC (mg/L)	6.87	3.63	10.44
UV_{254} (/cm)	0.102	0.032	0.114
pH	6.94	7.36	6.68
Mn (mg/L)	0.01	0.75	0.05
Al (mg/L)	0.01	0.01	0.06
Ca (mg/L)	21.91	30.76	46.53
Mg (mg/L)	0.99	10.25	10.98
Na (mg/L)	12.91	23.72	66.97
Fe (mg/L)	0.01	0.78	0.01
Cl^- (mg/L)	11.72	35.11	80.35
NO_3^- (mg/L)	1.73	0.19	3.09
SO_4^{2-} (mg/L)	21.14	8.4	56.83
PO_4^{3-} (mg/L)	0.99	0.54	1.25

Experiments were conducted under pseudo-first-order conditions [concentration of ferrate is in excess to ROX (10:1)], and the concentration changes of ferrate and ROX were recorded as a function of the reaction time (Eq (1)).

$$-d[ROX]/dt = k_{app}[ROX][ferrate]_{total} \quad (1)$$

Eq (2) shows the integral form of Eq (1),

$$\ln([ROX]t/[ROX]0) = -kapp\int_0^t [ferrate]dt \quad (2)$$

The pH-dependent change of k_{app} was interpreted by species-specific reaction between ferrate species ($H_3FeO_4^+ \Leftrightarrow H^+ + H_2FeO_4$, $pKa_1 = 1.5$; $H_2FeO_4 \Leftrightarrow H^+ + HFeO_4^-$, $pKa_2 = 3.5$; $HFeO_4^- \Leftrightarrow H^+ + FeO_4^{2-}$, $pKa_3 = 7.2$) (Sharma et al., 2001) and ROX species ($pKa_1 = 3.43$, $pKa_2 = 6.38$, $pKa_3 = 9.67$) (Chen and Huang, 2012) through Eq (3) and Eq (4).

$$d[ROX]_{total}/dt = - k_{app}\,[ferrate]_{total}[ROX]_{total}$$

$$= -\sum_{\substack{i=1,2,3\\ j=1,2,3}} k_{ij}\alpha_i\beta_j[ferrate]_{total}[ROX]_{total} \quad (3)$$

$$kapp = \sum_{\substack{i=1,2,3\\ j=1,2,3}} k_{ij}\alpha_i\beta_j \quad (4)$$

Where k_{app} is the apparent second-order rate constants for the reaction between ROX and ferrate. α_i and β_j are the molar fraction of ferrate and ROX; i and j represent the deprotonated ferrate species and ROX species, respectively. k_{ij} is the species-specific second-order rate constant for the reaction between the ferrate species i with ROX species j. When the pH value of the solution ranges from 6.5 to 10, the ferrate exists as $HFeO_4^-$ and FeO_4^{2-} in the system (Sharma, 2002), and pKa_2 (7.23) of ferrate is available for model fitting. Meanwhile, pKa_2 (6.38) and pKa_3 (9.67) of ROX are available for model fitting.

2.5. The desorption of As

Ferrate stock solution was separately added to 6 reactors containing 10 mM of $NaHCO_3$ buffered deionized water (pH = 7.0) and 5 μM of ROX (the molar ratio of Fe(VI)/ROX was 30:1). After reacting for 2 h, tiny yellow floc settled at the bottom of the solution. Three reactors were then spiked with NaCl, $MgCl_2$, and $Ca(NO_3)_2$ (end concentration: 10 mM) and reacted for 24 h. The pH value of 2 solution samples was adjusted by 50 mM HCl or 50 mM NaOH to pH 5.0 and 9.0, respectively, and reacted for 24 h. Another reactor was moved into water bath of 35 °C and reacted for 24 h. After that, the solution samples were analyzed to determine the variation of As content before and after desorption treatment.

2.6. Analytical methods

For SEM-EDX observations, the reaction solution containing ferric particles was filtered through hydrophilic acetate fiber membranes of 0.45 μm pore size (Shanghai ANPEL, China). The membranes were dried at 40 °C, sputter coated with gold, and observed with a Hitachi FE-SEM SU8000 (He et al., 2018). LC/ESI-QTOF-MS analysis was performed with a high-resolution hybrid quadrupole time-of-flight mass spectrometer (Q-TOF 5600, AB Sciex, USA) equipped with an electrospray ion (ESI) source. A 20 μL sample was injected to the source using a liquid chromatography (LC). Chromatographic separation was performed on a Thermo BDS Hypersil C18 column (4.6 mm × 150 mm, 5 μm particle size, Waltham, MA) maintaining at 30 °C. The mobile phase consisting of water (phase A) and acetonitrile (phase B) was eluted at a flow rate of 0.2 mL min^{-1}. The linear gradient was decreased from 100% A (2 min) to 95% A in 1 min, then maintained for 23 min, after returning to the starting condition in 1 min, and ended by an 8-min equilibration. Mass spectra (m/z 40-600) were recorded in negative ion mode using an electrospray ion (ESI) source with the ion source parameters described in previous study (Wang et al., 2016). The high-resolution LC-MS data were acquired with Analyst TF software (Version 1.6, AB Sciex) and processed using PeakView software (Version 1.2, AB Sciex).

3. Results and discussion

3.1. Effectiveness of ferrate on ROX and total As removal

Effectiveness of ferrate on ROX oxidation was initially explored (Fig. 1). When 5 μM of ROX reacted with 50 μM of ferrate at pH 7.0, more than 92% of ROX was removed by ferrate within 5 min. When the initial ferrate/ROX molar ratio increased to 20, almost complete removal of ROX was achieved within 40 s (the HPLC detection limit of ROX was 0.02 μM). According to published results, the reaction time is normally above 30 min for effective removal ($c/c_0 > 90\%$) of ROX with chemical oxidants or adsorbents (Acuña et al., 2017; Ji et al., 2016; Tian et al., 2017). This suggests that ferrate is highly effective for the oxidation of ROX.

Inorganic As species may be released during the transformation of ROX, and they are more toxic and mobile than ROX (Han et al., 2017). In the reaction with ROX, the effect of ferrate on total As removal was investigated (Fig. 1C). When 50 μM and 100 μM of ferrate reacted with 5 μM of ROX at pH 7.0, over 90% and 95% of the total As were removed within 30 min, respectively. When the ferrate/ROX molar ratio increased to 30, over 99% of total As were removed within 5 min, and the amount of total-As was below 10 μg/L, which satisfies the World Health Organization standard on the amount of As (below 10 μg/L) in drinking water.

3.2. Reaction kinetics

Second-order reaction rate law (Eq (1)) was used to study the reaction process. The reaction rate constants (k_{app}) were calculated based on natural logarithm of ROX concentrations and the relevant ferrate exposure ($\int_0^t [ferrate]dt$) values (Fig. 2A). The k_{app} values were 747 $M^{-1}s^{-1}$, 306 $M^{-1}s^{-1}$, and 111 $M^{-1}s^{-1}$ at pH 6.5, 7.0, and 7.5 respectively, and were 27 $M^{-1}s^{-1}$ to 1 $M^{-1}s^{-1}$ from pH 8.0 to pH 10. This suggests that the reaction was pH dependent, and ferrate was highly reactive with ROX under slightly acidic and neutral pH conditions. Chemically, the redox potential of ferrate is higher under acidic conditions than under basic conditions. Hence, acidic condition is in favor for the oxidation of ROX with ferrate. Besides, Joshi et al. reported that for the removal of aromatic organoarsenic compounds with metal oxides, the removal process was strongly pH dependent (Joshi et al. 2017a, 2017b). Low pH condition would make the adsorbents positively charged and increase the Coulombic electrostatic forces between adsorbents and aromatic organoarsenic compounds. This mechanism may also facilitate the removal of ROX with the ferrate resultant particles.

To further explore reaction mechanism, the measured rate constants k_{app} were compared with species-specific reaction model fitting [Eq (3) and Eq (4)] results, as shown in Fig. 2B. After model fitting, $k_{11} = (1.81 \pm 0.02) \times 10^3\ M^{-1}s^{-1}$, $k_{12} = (1.79 \pm 0.11) \times 10^2\ M^{-1}s^{-1}$, $k_{13} = k_{21} = k_{22} = k_{23} = 0$, and the model

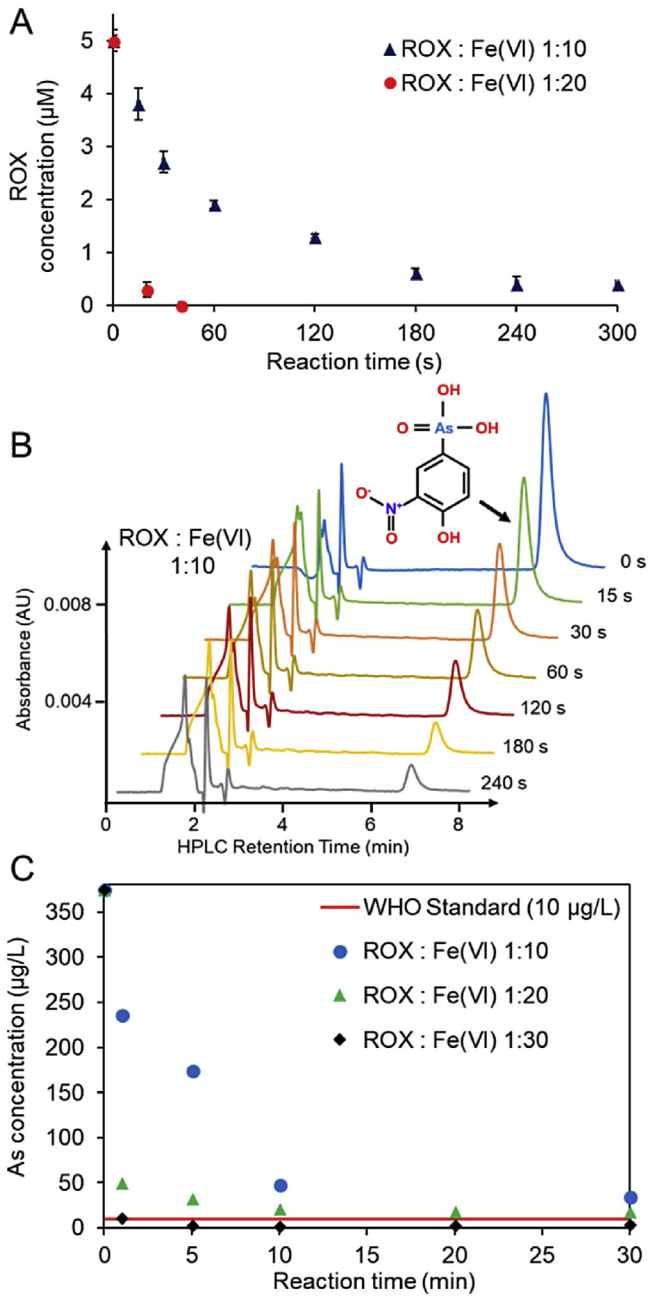

Fig. 1. Variation of ROX concentration under different initial ferrate/ROX molar ratios (A), HPLC spectrum of ROX reacts with ferrate (50 μM) (B), and variation of total-As in the reaction of ROX with ferrate as a function of reaction time (C). Experimental conditions: $[ROX]_0 = 5$ μM, T = 25 °C, pH = 7.0.

result is well fitted with measured reaction rate constants ($R^2 = 0.9997$). This indicates that i), in the reaction of ROX with ferrate, contribution of FeO_4^{2-} on ROX oxidation is negligible ($k_{21} = k_{22} = k_{23} = 0$); ii), $HFeO_4^-$ is the dominant ferrate specie reacting with ROX; iii), k_{11} is 10 times higher than k_{12}, which suggests that the reaction between $HFeO_4^-$ and deprotonated ROX controlled the overall reaction of ROX with ferrate from pH 6.5 to pH 10.

3.3. The conversion of As species

In the degradation of organoarsenicals, the released inorganic

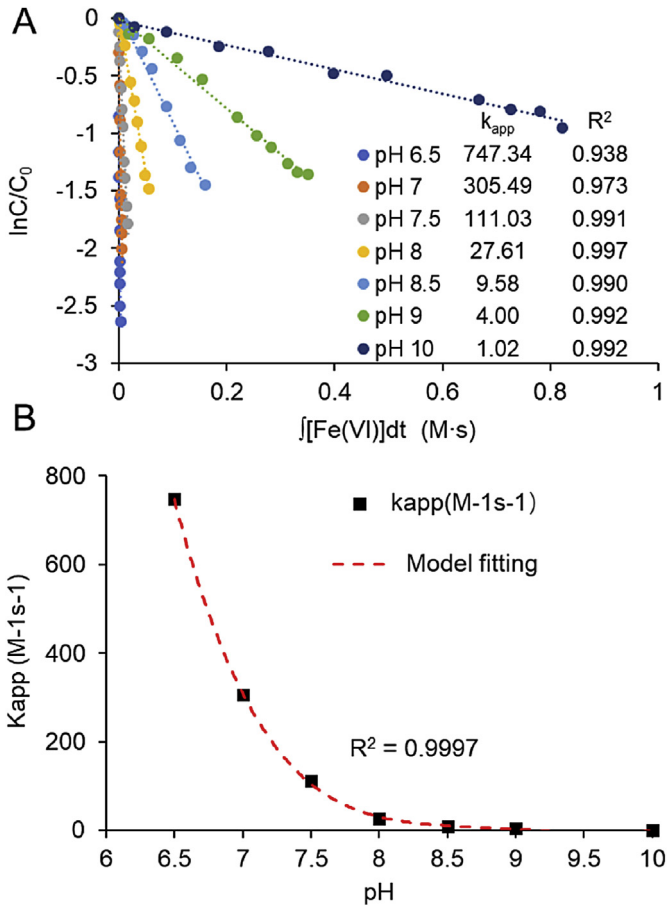

Fig. 2. Reaction kinetics of ferrate with ROX varies as a function of the exposure of ferrate under different pH conditions (A), and model fitting result of the second-order reaction rate constants of ROX with Fe(VI) varies as a function of solution pH (6.5–10) (B). Experimental conditions: $[ROX]_0 = 5$ μM, $[ferrate]_0 = 50$ μM, T = 25 °C.

arsenic is more toxic and mobile than its parent form. Conversion of As species in the reaction process was investigated. Fig. 3A shows the variation of ROX, total-As, As (III), and As (V) in the reaction process [hydroxylamine hydrochloride (1 mM) and HCl (v.t. 0.5%) were added to dissolve settled ferric floc]. The average concentration of total-As was around 5 μM during the experiment. This suggests that the total-As was mass balanced. Accordingly, the content of ROX decreased while the content of As (V) increased as a function of reaction time.

In the conversion of organoarsenicals, -$AsO(OH)_2$ group would be cleaved from aromatic ring, leading to the formation of AsO_3^{3-} (Czaplicka et al., 2014; Zhu et al., 2014). In the reaction of ROX with ferrate, we only observed traces of As(III) in LC-ICP-MS spectrum (Fig. 3B) in initial reaction stage (0–2 min), and the determined average amount of As (III) was 0.04 μM during the whole experiment. These data suggest that the -$AsO(OH)_2$ group was cleaved from ROX and may be further oxidized into As (V). Since toxicity and mobility of As (III) were higher than that of As (V), the conversion of ROX into As (V) was in favor for eliminating the toxicity of ROX. Meanwhile, the total As in the system could be effectively removed by ferrate (Fig. 1C).

The ferric nanoparticles formed in ferrate reduction have great potential on hazardous ion removal. Inorganic As (III) could be oxidized to As (V) by ferrate and subsequently removed by ferric coagulation (Lee et al., 2003b). Since the -$AsO(OH)_2$ group could be cleaved from ROX molecular and transformed into As(V), the *in situ*

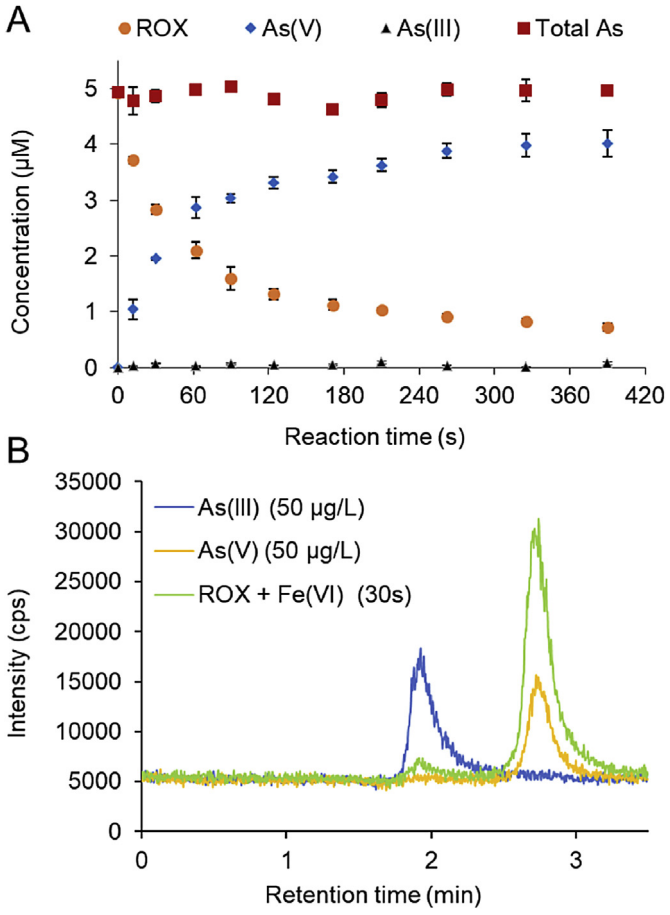

Fig. 3. Concentration variation of ROX, As(III), As(V), and total As in the reaction of ROX with ferrate (A), and LC-ICP − MS spectrum of As (III) standard, As (V) standard, and ROX treated by ferrate (B). Hydroxylamine hydrochloride (1 mM) and HCl (v.t. 0.5%) were added into the solution to dissolve the settled ferric floc before detection. Experimental conditions: T = 25 °C, $[ROX]_0$ = 5.0 μM, $[ferrate]_0$ = 50 μM, pH = 7.0.

formed ferric nanoparticles may further adsorb As(V). SEM-EDX and XPS analysis were employed to analyze the settled solids. The distribution of As in ferric particles is shown in Fig. 4. Generally, the settled solids are a mixture of Fe, Cl, C, K, Si, and As. The K, Cl, C, and Si found in the settled solids may come from the buffer solution, while the Fe and As originated from ferrate and ROX, respectively.

XPS analysis showed the chemical state of As in ROX samples before and after reaction with ferrate (Fig. 4C and D). Binding energy (BE) of fitting peak in ROX sample was 44.4 eV, which could be assigned to As(III) (44.3–44.5 eV). In comparison, the BE of fitting peak in solution settled solids (ferric particles) was 45.3 eV, which can be ascribed to As(V) (45.2–45.6 eV) (Chen et al., 2018; Zhang et al., 2007). These data suggested that following the reaction between ROX and ferrate, $AsO(OH)_2$ on ROX was oxidized to As(V) by ferrate. As(V) then reacted with *in situ* formed ferric nanoparticles (Prucek et al., 2013), and was removed by the ferrate resultant nanoparticles through particle aggregation and sedimentation.

3.4. Effect of solution pH on total As removal

Above results show that alkaline condition would negatively affect the oxidation of ROX by ferrate. Since arsenate would be formed in the ROX oxidation process, the effect of solution pH on total As removal was investigated. Fig. 5A shows the change of the total As removal ratio in the ROX oxidation process under different pH conditions. Over 99% of the total As was removed at pH 6.0, and the removal efficiency was relatively unchanged during the entire reaction process (120 min). Meanwhile, the concentration of Fe in solution was decreased from 2.8 mg/L to 0.08 mg/L within 1 min at pH 6.0 (Fig. 5B). These data suggest that ferrate has a strong reactivity with ROX and can effectively remove the released inorganic arsenic through Fe(III) formation under slightly acidic condition (pH 6.0). When the solution pH increased to 7.0, 53% of the total As were removed within 5 min, and over 90% of the total As were removed within 30 min. After that, the total As removal efficiency remained around 91%.

However, when the solution pH increased to 8.5 and 9.5, the total As removal efficiencies were below 7% in both groups. Alkaline conditions would enhance the stability of ferrate and the concentration of dissolved Fe was above 2.3 mg/L throughout the reaction in the groups. This indicates that less than 18% of ferrate was transformed into particles through the experiment. Since the ferrate resultant nanoparticles were critical for the removal of the inorganic As species, high level of ferrate stability would impact the removal of the total As in the reaction.

Solution pH not only affects the stability of ferrate, but also influences the surface charge of relevant particles. For the ferric nanoparticles formed in ferrate reduction process, their zero-potential point was 6.8 (Liu et al., 2017). The ferrate resultant particles were negatively charged under alkaline condition. This can impact the particle aggregation behavior and affect the removal of total As. Besides, the organoarsenicals and inorganic arsenics were negatively charged under pH 6.0–10.0 (Sun et al., 2017). The electrostatic repulsion between ferric nanoparticles and As species may also impact the removal of As with ferrate.

3.5. Oxidation products and reaction pathway

In above sections we showed that ROX could be effectively oxidized by ferrate and that the released inorganic As species could be eliminated by ferrate resultant particles. However, transformation of aromatic ring part of ROX is ambiguous. HPLC/ESI-QTOF-MS was employed to analyze the oxidation products of ROX. By comparing TIC chromatograms before and after the reaction of ROX with ferrate, chromatographic peak of ROX appearing at 27.8 min was initially identified (Fig. 6A and 6B). The intensity of ROX chromatographic peak largely decreased after 2 min of reaction. This is in accordance with above data that ferrate is effective for the oxidation of ROX.

Besides ROX, several new peaks appear in the TIC chromatogram after 2 min of reaction. Three possible oxidation products were obtained from the HPLC/ESI-QTOF-MS results. The m/z of Product 1 is 154.95 Da (Fig. 6C). After analyzing the possible degradation pathway of ROX, we speculate that Product 1 was 2-nitrohydroquinone. In the reaction of ferrate with ROX, ferrate initially attracts the As–C bond of ROX. Oxygen atoms were transferred from ferrate to ROX, leading to the oxidation of $-AsO(OH)_2$ group into arsenic acid (Fig. 4). In this process, the aromatic ring in ROX was oxidized by ferrate and transformed into 2-nitrohydroquinone (Fig. 7). Besides Product 1, Product 2 (m/z = 152.03) also showed intense signal in the TIC chromatograms. After analyzing the ionization pattern of Product 2, we speculate it may be nitro-1,4-benzoquinone, a transformation product of 2-nitrohydroquinone (Fig. 7). Chemically, the nitro-1,4-benzoquinone is difficult to ionize. However, some double bonds are reduced in the electrospray ionization process, leading to the formation of the ionized product.

The arsenic ion further reacted with ferrate and would be removed by ferrate resultant nanoparticles, as discussed in

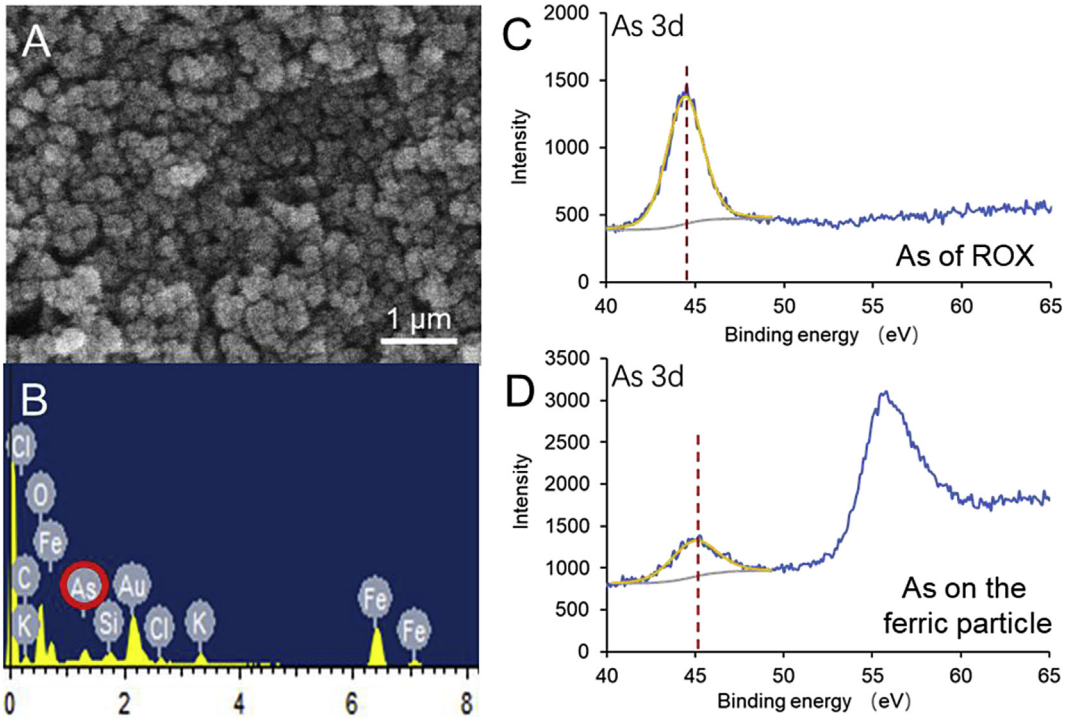

Fig. 4. SEM (A) photo and EDX analysis result (B) of settled solids formed in the reaction of ROX with ferrate, and As 3d core level photoelectron spectra of ROX (C) and the settled solids (D). Experimental conditions: T = 25 °C, $[ROX]_0$ = 5.0 μM, $[ferrate]_0$ = 50 μM, pH = 7.0.

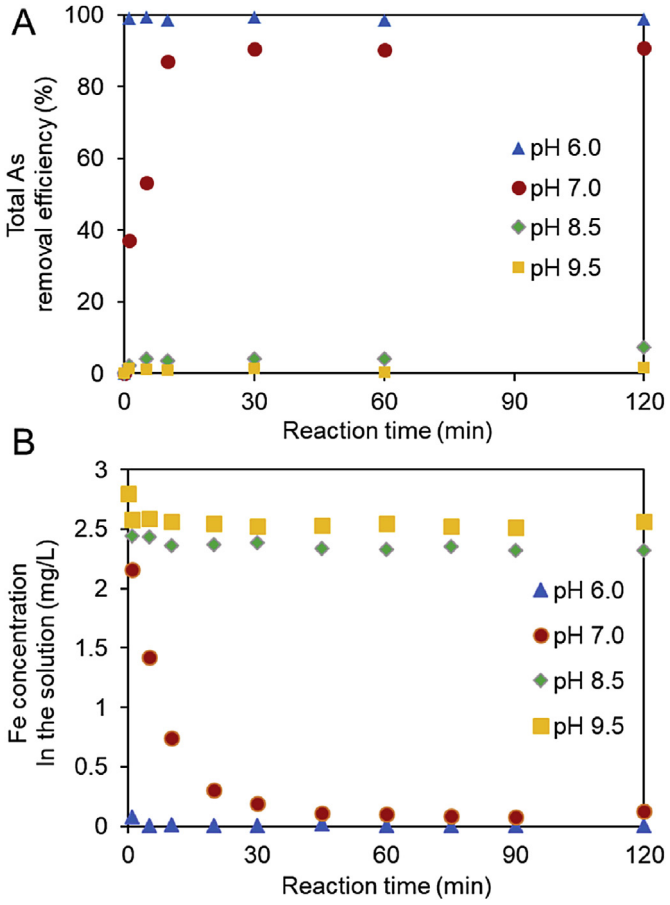

Fig. 5. Removal of total As (A) and concentration change of Fe (B) as a function of reaction time under different pH conditions. Experimental conditions: T = 25 °C, $[ROX]_0 = 5.0\ \mu M$, $[ferrate]_0 = 50\ \mu M$.

previous sections. On the other hand, 2-nitrohydroquinone and nitro-1,4-benzoquinone may be further oxidized by ferrate, leading to the formation of product 3 ($m/z = 96.96$, Fig. 6D). We noticed that this product also appeared in the mass spectrum of ROX. We speculated that it is phenol, but the molecular weight of phenol is 94.11 (Fig. 6E). Product 3 may be a ring cleavage product of nitro-1,4-benzoquinone (Fig. 7).

The variations of relative intensity of ROX and the products identified during oxidation are recorded (Fig. 8). In accordance with the proposed mechanism, the intensity of Product 1 increased with the decrease of ROX at the beginning of reaction. This indicates that Product 1 may be a primary oxidation product formed at the initial stage of the ferrate oxidation of ROX. After one minute, the intensity of Product 1 decreased, as that of Product 2 increased at the same time. This suggests Product 1 was further oxidized. After two minutes, the intensity of Product 2 decreased, while that of Product 3 increased significantly. Such change is in accordance with the proposed mechanism (Fig. 8), where ROX and successive oxidation products are oxidized by ferrate, resulting in ring cleavage products in the system.

3.6. Aggregation of ferric particles and desorption of As from settled floc

For the removal of hazardous ions with adsorbent, environmental factors such as water temperature, background ions, and solution pH would affect the interaction between target pollutants and adsorbent, thus lead to the desorption of captured hazardous ions. Ferrate resultant particles adsorbed As species releasing from ROX. Background constituents would competitively combine with ferric particles and influence their chemical properties, and this may make the captured As species desorbed. Desorption of captured As species would greatly impact the water quality. Hence, the aggregation behavior of As-bearing ferric particles and the desorption of As species from ferric floc were investigated.

The average hydrodynamic diameter of the ferric particles was around 170 nm, and this average diameter surpassed 1 μm within 40 min under static condition (Fig. 9A). After 2 h, the average diameter surpassed 1.5 μm. These data showed that the hydrodynamic size of ferrate resultant particles would increase from nanoscale to micrometer-scale within an hour. When coagulant was added and the solution was vigorously stirred, the ferric particles are swiftly expanding and captured by coagulant. The rapid expansion of particle size would facilitate the separation of As-bearing ferric particles in relevant treatment procedures.

Effects of background ions (Na^+, Mg^{2+}, Ca^{2+}, Cl^-, and NO_3^-) and decreasing solution pH (from pH 7.0 to 5.0) on the desorption of As were not remarkable, while increase in solution temperature and pH noticeably led to the desorption of As (Fig. 9B). The As(V) formed in ROX degradation process was removed by ferrate resultant particles. The combination of As species and ferric particles can resist the negative effects of background ions on the desorption of As. In comparison, elevating solution temperature would increase the energy of the system, attenuate the interaction of As and ferric particles and thus lead to the desorption of adsorbed As.

When solution pH decreased from 7.0 to 5.0, no As desorption was observed. In comparison, when solution pH increased to 9.0, the level of desorbed As surpassed 70 μg/L, much higher than the WHO regulated As contained (10 μg/L) in drinking water. As species mainly exist as anion of AsO_4^{3-} and AsO_3^{3-} in water, and the isoelectric point (pH_{pzc}) of ferrate resultant particles were 6.8. The electrostatic attraction between anion and positively charged particles is in favor for the removal of As species with ferric floc at circumneutral pH. However, when solution pH increased to 9.0, the OH^- competed with adsorbed As species for the interaction with ferric particles, and this process led to desorption of captured As. Hence, for the removal of ROX in authentic polluted waters, monitoring the variation in solution pH and temperature, and regularly removing settled floc can prevent desorption of As.

3.7. Oxidation of ROX and total-As removal in authentic waters

Background constituents existing in authentic waters would affect aggregation behavior and physical properties of nanoparticle (Liu et al., 2018), and may influence the removal of As. Ferrate oxidation of ROX in authentic waters was investigated. Fig. 10A shows the concentration changes of ROX when reacting with ferrate in river water, ground water and WWTP effluent (ferrate/ROX molar ratio is 20:1). ROX was removed within 2 min in ground water and 3 min in river water, respectively. In comparison, merely 85% of ROX was removed in WWTP effluent after 20 min of reaction. Compared with that in river water and ground water, the removal of ROX in WWTP effluent was largely affected. According to the characteristics of water samples, the content of organic substance (TOC), Ca^{2+}, Na^+, Cl^-, SO_4^{2-}, and PO_4^{3-} in WWTP effluent is 0.5–8 times higher than that in river water and ground water (Table 1). Organic constituents in authentic waters may competitively consume ferrate and decrease the oxidation of ROX in the system. Co-existing species such as Ca^{2+}, Na^+, Cl^-, SO_4^{2-}, and PO_4^{3-} also influence the activity of ferrate (Wang et al., 2018) and thus obstruct the removal of ROX. However, compared with published methods on ROX control, ferrate oxidation is effective for removal

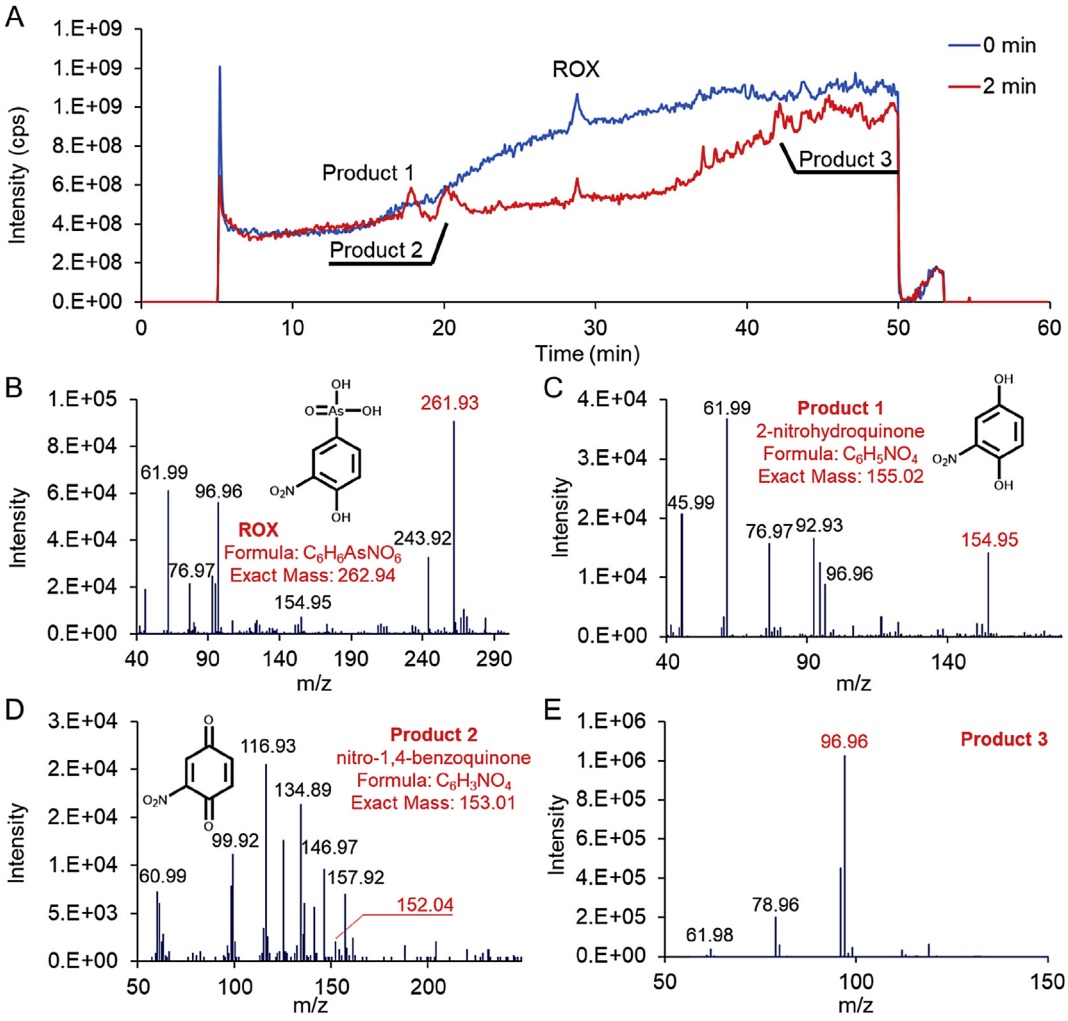

Fig. 6. TIC chromatograms of ROX oxidized by ferrate at different reaction time (A), and MS/MS spectrum of ROX (B), 2-nitrohydroquinone (C), nitro-1,4-benzoquinone (D) and another possible degradation product of ROX (E). Experimental conditions: $[ROX]_0 = 5\ \mu M$, $[ferrate]_0 = 50\ \mu M$, $T = 25\ ^\circ C$, pH 7.0.

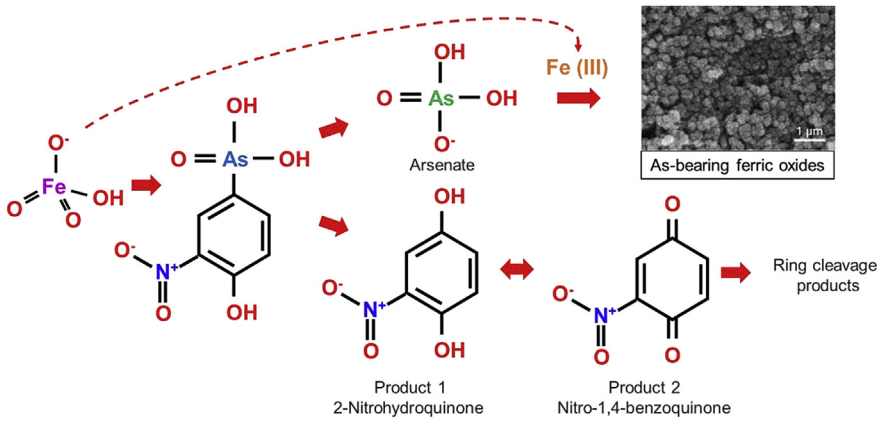

Fig. 7. Proposed reaction mechanism about the ferrate oxidation of ROX.

of ROX under circumneutral pH conditions (Acuña et al., 2017; Chen and Huang, 2012; Ji et al., 2016).

Although the ROX oxidation ratio was affected, total As removal ratios in three groups surpassed 86% within half an hour (Fig. 10B). The removal of As species could be attributed to the function of ferric particles. Although background constituents affected oxidation behavior of ferrate, the adsorption ability of ferrate resultant ferric particles towards As species was not greatly affected. Ferrate is highly effective to remove total-As for the treatment of ROX in authentic waters.

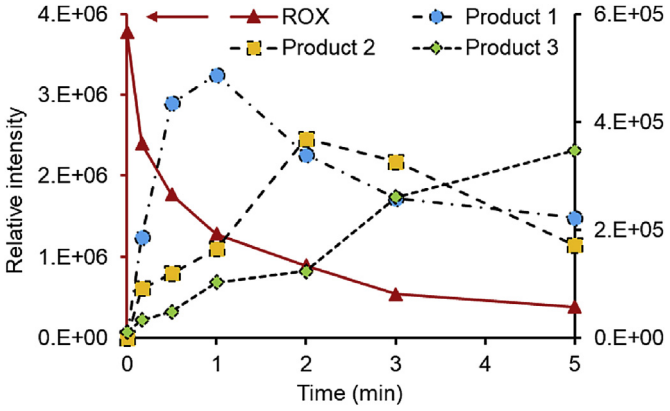

Fig. 8. Variation of relative intensity of ROX and the identified oxidation products as a function of reaction time.

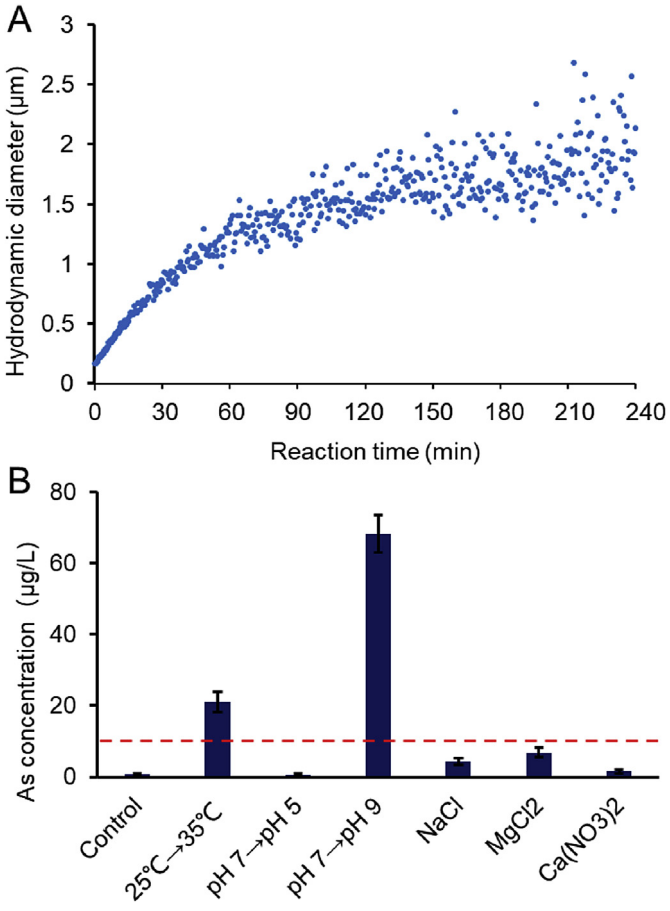

Fig. 9. Aggregation profile of ferric particles formed in reaction of ROX (5 μM) with ferrate (50 μM) (A), and effects of elevating solution temperature, adjusting pH, and adding 10 mM co-existing ions on the concentration of total-As after 24 h treatment (ROX = 5 μM, initial ferrate/ROX ratio = 30: 1) (B).

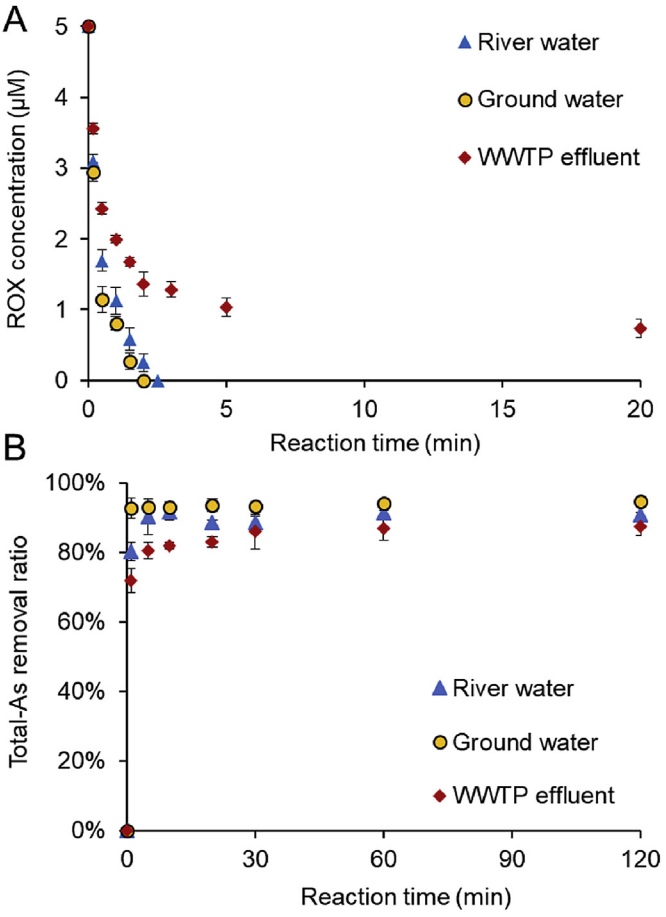

Fig. 10. Concentration change of ROX treated by ferrate in river water, ground water and WWTP effluent as a function of reaction time (A), and total As removal ratios varies in the reaction process (B). Experimental conditions: T = 25 °C, $[ROX]_0$ = 5.0 μM, $[ferrate]_0$ = 100 μM, pH = 7.0.

4. Conclusions

This work explored the oxidation of ROX with ferrate and examined the transformation of As species in reaction process. Following conclusions are drawn.

1. Ferrate can rapidly oxidize ROX under neutral pH condition. At pH 7.0, the reaction rate constant of ferrate with ROX was 305 $M^{-1}s^{-1}$. The apparent second-order rate constants of ferrate with ROX ranged from 747 to 1 $M^{-1}s^{-1}$ when solution pH increased from 6.5 to 10.
2. The total-As in the system could be effectively removed after ferrate treatment. When initial ferrate/ROX molar ratio was 20, over 95% of total As would be removed within 10 min under pH 7.0; When the molar ratio increased to 30, 96% of total As would be removed within 1 min.
3. As—C bond would be attacked by ferrate, leading to the cleavage of -$AsO(OH)_2$ group. The -$AsO(OH)_2$ group would be oxidized into As(V) and subsequently removed by *in situ* formed ferric nanoparticles.
4. The aromatic ring part of ROX would be oxidized by ferrate, leading to the formation of 2-nitrohydroquinone and nitro-1,4-benzoquinone. These products may be further oxidized into ring cleavage product or reduction product of phenol.
5. Ferrate could effectively oxidize ROX and remove total As in authentic waters.

Acknowledgments

This work was financially supported by the National Key R&D Program of China (2017YFA0207203), the National Natural Science Foundation of China (Grant No. 51808163), the State Key Laboratory

of Urban Water Resource and Environment (Harbin Institute of Technology) (NO.2016DX04), and the HIT Environment and Ecology Innovation Special Funds (HSCJ201605).

References

Acuña, K., Yáñez, J., Ranganathan, S., Ramírez, E., Cuevas, J.P., Mansilla, H.D., Santander, P., 2017. Photocatalytic degradation of roxarsone by using synthesized ZnO nanoplates. Sol. Energy 157, 335–341.

Adak, A., Mangalgiri, K.P., Lee, J., Blaney, L.M., 2015. UV irradiation and UV-H2O2 advanced oxidation of the roxarsone and nitarsone organoarsenicals. Water Res. 70, 74–85.

Bednar, A.J., Garbarino, J.R., Ferrer, I., Rutherford, D.W., Wershaw, R.L., Ranville, J.F., Wildeman, T.R., 2003. Photodegradation of roxarsone in poultry litter leachates. Sci. Total Environ. 302, 237–245.

Chapman, H., Johnson, Z., 2002. Use of antibiotics and roxarsone in broiler chickens in the USA: analysis for the years 1995 to 2000. Poultry Sci. 81 (3), 356–364.

Chen, J., Wang, J., Zhang, G., Wu, Q., Wang, D., 2018. Facile fabrication of nanostructured cerium-manganese binary oxide for enhanced arsenite removal from water. Chem. Eng. J. 334, 1518–1526.

Chen, W., Huang, C., 2012. Surface adsorption of organoarsenic roxarsone and arsanilic acid on iron and aluminum oxides. J. Hazard Mater. 227, 378–385.

Czaplicka, M., Bratek, Ł., Jaworek, K., Bonarski, J., Pawlak, S., 2014. Photo-oxidation of p-arsanilic acid in acidic solutions: kinetics and the identification of by-products and reaction pathways. Chem. Eng. J. 243, 364–371.

Fan, J., Lin, B.-H., Chang, C.-W., Zhang, Y., Lin, T.-F., 2018. Evaluation of potassium ferrate as an alternative disinfectant on cyanobacteria inactivation and associated toxin fate in various waters. Water Res. 129 (Suppl. C), 199–207.

Feng, M., Wang, X., Chen, J., Qu, R., Sui, Y., Cizmas, L., Wang, Z., Sharma, V.K., 2016. Degradation of fluoroquinolone antibiotics by ferrate(VI): effects of water constituents and oxidized products. Water Res. 103 (Suppl. C), 48–57.

Garbarino, J.R., Bednar, A.J., Rutherford, D.W., Beyer, R.S., Wershaw, R.L., 2003. Environmental fate of roxarsone in poultry litter. I. Degradation of roxarsone during composting. Environ. Sci. Technol. 37 (8), 1509–1514.

Graham, N.J.D., Jiang, C., Li, X., Jiang, J.Q., Ma, J., 2004. The influence of pH on the degradation of phenol and chlorophenols by potassium ferrate. Chemosphere 56 (10), 949–956.

Guo, Q., Liu, L., Hu, Z., Chen, G., 2013. Biological phosphorus removal inhibition by roxarsone in batch culture systems. Chemosphere 92 (1), 138–142.

Han, J.-C., Zhang, F., Cheng, L., Mu, Y., Liu, D.-F., Li, W.-W., Yu, H.-Q., 2017. Rapid release of arsenite from roxarsone bioreduction by exoelectrogenic bacteria. Environ. Sci. Technol. Lett. 4 (8), 350–355.

He, C., Li, X.-z., Sharma, V.K., Li, S.-y., 2009. Elimination of sludge odor by oxidizing sulfur-containing compounds with ferrate (VI). Environ. Sci. Technol. 43 (15), 5890–5895.

He, H., Liu, Y., Wang, X., Huang, Z., Xu, C., Yang, T., Zhang, Z., Wang, L., Ma, J., 2018. Effects of newly prepared alkaline ferrate on sludge disintegration and methane production: reaction mechanism and model simulation. Chem. Eng. J. 343, 520–529.

Hu, P., Liu, Y., Jiang, B., Zheng, X., Zheng, J., Wu, M., 2015. High-efficiency simultaneous oxidation of organoarsenic and immobilization of arsenic in Fenton enhanced plasma system. Ind. Eng. Chem. Res. 54 (33), 8277–8286.

Hu, Y., Zhang, W., Cheng, H., Tao, S., 2017. Public health risk of arsenic species in chicken tissues from live poultry markets of guangdong province, China. Environ. Sci. Technol. 51 (6), 3508–3517.

Ji, Y., Shi, Y., Kong, D., Lu, J., 2016. Degradation of roxarsone in a sulfate radical mediated oxidation process and formation of polynitrated by-products. RSC Adv. 6 (85), 82040–82048.

Jiang, J., 2007. Research progress in the use of ferrate (VI) for the environmental remediation. J. Hazard Mater. 146 (3), 617–623.

Joshi, T.P., Zhang, G., Cheng, H., Liu, R., Liu, H., Qu, J., 2017a. Transformation of para arsanilic acid by manganese oxide: adsorption, oxidation, and influencing factors. Water Res. 116 (Suppl. C), 126–134.

Joshi, T.P., Zhang, G., Jefferson, W.A., Perfilev, A.V., Liu, R., Liu, H., Qu, J., 2017b. Adsorption of aromatic organoarsenic compounds by ferric and manganese binary oxide and description of the associated mechanism. Chem. Eng. J. 309, 577–587.

Lee, Y., Um, I.-h., Yoon, J., 2003a. Arsenic (III) oxidation by iron (VI)(ferrate) and subsequent removal of arsenic (V) by iron (III) coagulation. Environ. Sci. Technol. 37 (24), 5750–5756.

Lee, Y., Um, I., Yoon, J., 2003b. Arsenic(III) oxidation by iron(VI) (ferrate) and subsequent removal of arsenic(V) by iron(III) coagulation. Environ. Sci. Technol. 37 (24), 5750–5756.

Lee, Y., Yoon, J., Von Gunten, U., 2005. Kinetics of the oxidation of phenols and phenolic endocrine disruptors during water treatment with ferrate (Fe (VI)). Environ. Sci. Technol. 39 (22), 8978–8984.

Li, B., Zhu, X., Hu, K., Li, Y., Feng, J., Shi, J., Gu, J., 2016. Defect creation in metal-organic frameworks for rapid and controllable decontamination of roxarsone from aqueous solution. J. Hazard Mater. 302, 57–64.

Liu, X., Zhang, W., Hu, Y., Hu, E., Xie, X., Wang, L., Cheng, H., 2015. Arsenic pollution of agricultural soils by concentrated animal feeding operations (CAFOs). Chemosphere 119, 273–281.

Liu, Y., Wang, L., Huang, Z., Wang, X., Zhao, X., Ren, Y., Sun, S., Xue, M., Qi, J., Ma, J., 2018a. Oxidation of odor compound indole in aqueous solution with ferrate (VI): kinetics, pathway, and the variation of assimilable organic carbon. Chem. Eng. J. 331, 31–38.

Liu, Y., Wang, L., Ma, J., Zhao, X., Huang, Z., Mahadevan, G.D., Qi, J., 2016. Improvement of settleability and dewaterability of sludge by newly prepared alkaline ferrate solution. Chem. Eng. J. 287, 11–18.

Liu, Y., Wang, L., Wang, X., Huang, Z., Xu, C., Yang, T., Zhao, X., Qi, J., Ma, J., 2017. Highly efficient removal of trace thallium from contaminated source waters with ferrate: role of in situ formed ferric nanoparticle. Water Res. 124 (Suppl. C), 149–157.

Liu, Y., Yang, T., Wang, L., Huang, Z., Li, J., Cheng, H., Jiang, J., Pang, S., Qi, J., Ma, J., 2018. Interpreting the effects of natural organic matter on antimicrobial activity of Ag2S nanoparticles with soft particle theory. Water Res. 145 (15), 12–20.

Ma, J., Liu, W., 2002. Effectiveness and mechanism of potassium ferrate (VI) preoxidation for algae removal by coagulation. Water Res. 36 (4), 871–878.

Prucek, R., Tuček, J., Kolařík, J., Filip, J., Marušák, Z., Sharma, V.K., Zbořil, R., 2013. Ferrate(VI)-Induced arsenite and arsenate removal by in situ structural incorporation into magnetic iron(III) oxide nanoparticles. Environ. Sci. Technol. 47 (7), 3283–3292.

Rush, J.D., Bielski, B.H., 1986. Pulse radiolysis studies of alkaline iron (III) and iron (VI) solutions. Observation of transient iron complexes with intermediate oxidation states. J. Am. Chem. Soc. 108 (3), 523–525.

Sarmah, A.K., Meyer, M.T., Boxall, A.B., 2006. A global perspective on the use, sales, exposure pathways, occurrence, fate and effects of veterinary antibiotics (VAs) in the environment. Chemosphere 65 (5), 725–759.

Sharma, V.K., 2002. Potassium ferrate (VI): an environmentally friendly oxidant. Adv. Environ. Res. 6 (2), 143–156.

Sharma, V.K., Oconnor, D.B., Cabelli, D.E., 2001. Sequential one-electron reduction of Fe(V) to Fe(III) by cyanide in alkaline medium. J. Phys. Chem. B 105 (46), 11529–11532.

Stolz, J.F., Perera, E., Kilonzo, B., Kail, B., Crable, B., Fisher, E., Ranganathan, M., Wormer, L., Basu, P., 2007. Biotransformation of 3-nitro-4-hydroxybenzene arsonic acid (roxarsone) and release of inorganic arsenic by Clostridium species. Environ. Sci. Technol. 41 (3), 818–823.

Sun, T., Zhao, Z., Liang, Z., Liu, J., Shi, W., Cui, F., 2017. Efficient degradation of p-arsanilic acid with arsenic adsorption by magnetic CuO-Fe 3 O 4 nanoparticles under visible light irradiation. Chem. Eng. J.

Thornton, P.K., 2010. Livestock production: recent trends, future prospects. Philos. Trans. R. Soc. Lond. B Biol. Sci. 365 (1554), 2853–2867.

Tian, C., Zhao, J., Zhang, J., Chu, S., Dang, Z., Lin, Z., Xing, B., 2017. Enhanced removal of roxarsone by Fe 3 O 4@ 3D graphene nanocomposites: synergistic adsorption and mechanism. Environ. Sci.: Nano 4 (11), 2134–2143.

Wang, L., Liu, Y., Ma, J., Zhao, F., 2016. Rapid degradation of sulphamethoxazole and the further transformation of 3-amino-5-methylisoxazole in a microbial fuel cell. Water Res. 88, 322–328.

Wang, X., Liu, Y., Huang, Z., Wang, L., Wang, Y., Li, Y., Li, J., Qi, J., Ma, J., 2018. Rapid oxidation of iodide and hypoiodous acid with ferrate and no formation of iodoform and monoiodoacetic acid in the ferrate/I−/HA system. Water Res. 144, 592–602.

Xie, X., Hu, Y., Cheng, H., 2016. Mechanism, kinetics, and pathways of self-sensitized sunlight photodegradation of phenylarsonic compounds. Water Res. 96, 136–147.

Yang, B., Ying, G.-G., 2013. Oxidation of benzophenone-3 during water treatment with ferrate(VI). Water Res. 47 (7), 2458–2466.

Yang, B., Ying, G.-G., Zhao, J.-L., Liu, S., Zhou, L.-J., Chen, F., 2012. Removal of selected endocrine disrupting chemicals (EDCs) and pharmaceuticals and personal care products (PPCPs) during ferrate(VI) treatment of secondary wastewater effluents. Water Res. 46 (7), 2194–2204.

Zhang, G.-S., Qu, J.-H., Liu, H.-J., Liu, R.-P., Li, G.-T., 2007. Removal mechanism of as (III) by a novel Fe– Mn binary oxide adsorbent: oxidation and sorption. Environ. Sci. Technol. 41 (13), 4613–4619.

Zhu, X.-D., Wang, Y.-J., Liu, C., Qin, W.-X., Zhou, D.-M., 2014. Kinetics, intermediates and acute toxicity of arsanilic acid photolysis. Chemosphere 107, 274–281.